CHAPTER 185

Hydrodynamic Characteristics of Wave-power-extracting Caisson Breakwater

Shigeo Takahashi*

ABSTRACT

The wave power extracting caisson breakwater can convert the wave energy into usable energy. The function and the stability of the caisson as a breakwater are investigated experimentally. It is found that wave reflection and wave transmission of the breakwater are relatively small and that the stability of the breakwater caisson against storm waves is high. The design method of the caisson is proposed considering the impact air pressure in the air chamber.

1. INTRODUCTION

Perforated wall caissons are increasingly adopted as the structures of seawalls and breakwaters since Jarlan (1961) invented the perforated wall caisson. This is because the perforated wall caissons have low wave reflection and overtopping characteristics, and is highly stable due to their wave absorbing capability. The wave power extracting caisson breakwater such as the one illustrated in Fig.1 is a kind of the perforated wall caisson because it can absorb the wave energy. However the wave power extracting caisson can actually convert the wave energy into usable energy. The converted energy can be used for many purpose in the sea and in the land near the breakwater.

This breakwater is consisted of the wave power extracting caisson on a rubble foundation. The caisson has an air chamber which is attached to the ordinary caisson. The waves enter into the air chamber from the opening under the front curtain wall, and cause the vertical oscillation of the water surface in the air chamber. Then the air in the upper half of the air chamber is

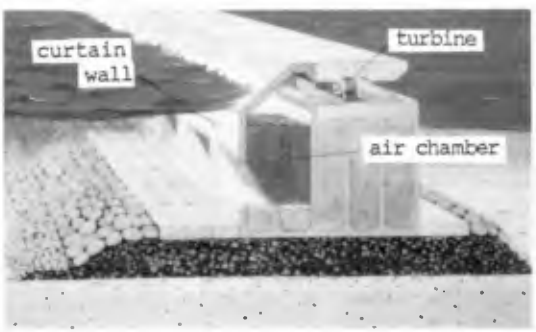

Fig.1 Wave Power Exracting Caisson Breakwater

* Chief of Maritime Structures Lab., Port and Harbor Res. Inst., 3-1-1, Nagase, Yokosuka, Japan 239

compressed and is expanded. The air motion generates the high-velocity flow through the nozzle which activates the air turbine and generates electricity. Thus the caisson functions as a wave power converter. A combination of the wave power converter and the vertical breakwater is attractive from the viewpoint of economical feasibility of wave power extraction, because the construction cost can be jointly borned by the accounts for power generation and harbour protection.

The studies on the wave power conversion have been conducted and the design of the caisson as a wave power converter has already been established(Ojima 1984, Takahashi 1986, 1987). In the present paper, the function and the stability of the caisson as a breakwater are investigated.

2. THEORY OF WAVE POWER CONVERSION

The conversion efficiency from wave power to air power in the air chamber is the most important factor not only as a wave power converter but also as a breakwater, because the higher conversion efficiency yields the lower wave reflection and transmission coefficient, and probably yields the higher stability.

The theory of wave power conversion by the wave power extracting caisson was originally given by Ojima et al.(1984) and was extended by Takahashi et al.(1987). The theory was named as **the thermodynamics and wave kinematics method.** The theory comprises two thermodynamics equations in the air chamber and one wave-kinematics equation at the air chamber opening under the curtain wall as follows:

$$\frac{dp^*}{dt} = \gamma \frac{p^*+p_0}{D_0-\eta}\left\{\frac{d\eta}{dt} - c_d \varepsilon w_p\right\} \tag{1}$$

$$\frac{dT^*}{dt} = \frac{T^*+T_0}{D_0-\eta}\left\{-\frac{d\eta}{dt} + \frac{D_0-\eta}{p^*+p_0}\frac{dp^*}{dt} + c_d \varepsilon w_p\right\} \tag{2}$$

$$2\eta_I = \frac{1}{\rho_w g} f(kh,\ kd_c) p^* + \frac{kB}{\tan kB}\eta + \frac{kB}{\sigma}\frac{d\eta}{dt}\frac{1}{\cos\theta_M} \tag{3}$$

The main unknown variables of the equations are

- p^* : oscillating fraction of the air pressure inside the air chamber
- η : oscillating fraction of the water surface elevation
- T^* : oscillating fraction of the air temperature inside the air chamber

The air flow velocity w_p in the air nozzle on the air chamber is defined by

$$w_p = \pm \varphi \sqrt{\frac{2}{\rho_a}} \sqrt{|p^*|} \tag{4}$$

The term $f(kh,kd_c)$ is given by

$$f(kh,\ kd_c) = \frac{2\cosh kh \sinh k(h-d_c)}{\cosh k(h-d_c)\sinh k(h-d_c) + k(h-d_c)} \tag{5}$$

The above equations can be solved by step-by-step numerical calculations when the following dimensions and characteristics of the incident waves and the air chamber are given:

η_I : incident wave profile
σ : wave angular frequency for the significant wave period
k : wave number for the significant wave period
θ_M : instantaneous wave angle
h : water depth
B : width of the air chamber
D_o : height of the air chamber above the still water level
d_c : submerged depth of the front curtain wall
A_w : nozzle opening area
ε : nozzle opening ratio (= $A_w/l_B B$)
l_B : length of air chamber in the breakwater direction
c_d : contraction coefficient of the nozzle (= 1.0 in the calculations)
φ : nozzle velocity coefficient

The constants in the equations are

γ : specific heat ratio (= 1.4)
ρ_w : density of water (= 1030 kg/m^3 in salt water)
g : gravity acceleration (9.8 m/s^2)
ρ_a : density of air (= 1.225 kg/m^3)
T_a : temperature in open air (15 C = 288 K)
p_a : pressure in open air (1 atm = 1.013x10^{5}N/m^2)

The wave power W_I is converted into air power. The instantaneous air power W_a, the average air power $\bar{W}_a$ and the conversion efficiency $\overline{EFF}_a$ are expressed by

$$W_a = p * w_p A_w \tag{6}$$

$$\bar{W}_a = \frac{1}{T_L}\int_0^{T_L} W_a\, dt \tag{7}$$

$$\overline{EFF}_a = \bar{W}_a / \bar{W}_I \ell_B \tag{8}$$

where T_L is the time duration of the wave action.

The theory mentioned above describes only the conversion from wave power to air power by the air chamber with an air nozzle. When a turbine and a generator are installed instead of the nozzle an equation of motion of the turbine and generator should be given and the characteristics and dimensions of the nozzle should be replaced by those of the turbine. However only the conversion from wave power to air power is discussed in this paper.

3. EXPERIMENTS

A series of model experiments were conducted in a large wave

flume. Four caisson breakwaters were tested in the experiments, namely,
a) Wave power extracting caisson with a sloped front face as in Fig.2(a), (named as the S-type caisson and denoted by WPEC-S),
b) Wave power extracting caisson with a vertical front face as in Fig.2(b), (the V-type caisson , WPEC-V),
c) Ordinary caisson with a sloped front face, (the sloped front wall caisson, SFWC),
d) Ordinary caisson covered with wave dissipating blocks as in Fig.2(c), (the caisson with wave dissipating blocks, SFWC-B).

The S-type caisson was the main caisson in the experiments and the V-type caisson was employed to compare the function and the stability by the difference of the air chamber shape. The V-type caisson was used in the previous studies on the wave power conversion. The S-type caisson was designed to improve the characteristics of the V-type caisson. The two other caissons were also examined to compare the hydrodynamic characteristics with those of the wave power extracting caissons.

The S-type caisson has a width B_t of 135 cm, a crown height h_c of 55 cm, a caisson depth h' of 80 cm and an air chamber width B of 35 cm. The front wall is inclined 45 degrees from the point 2.5 cm above the still water level. The armour units for the rubble foundation have a weight of 1.23 kgf each. The foot protection concrete block has a height of 7.5 cm and a width of 22.5 cm. The submerged depth d_c of the curtain wall of the caisson is 20 cm in the figure. The submerged depth was changed to 15 cm and 25 cm by changing the curtain wall plate. The caisson has an air nozzle with a diameter and length of 4.70 cm and 5.7 cm. The opening ratio ε of the nozzle to the horizontal area in the air chamber is 0.0075.

The air chamber width of S-type caisson is set at 13 % of the wavelength for T = 1.34 s. The air chamber width and the opening ratio are set to have a relatively high conversion efficiency with a small air chamber width. These values are dependent on the wave and other conditions and should be selected considering the whole wave conversion system. The submerged depth of the curtain wall is determined to be about 0.25 H_{max}. The upper deck of the turbine room is design to be higher than 0.5 H_{max}. The crown height of the caisson is designed to be 1.0 $H_{1/3}$. The values of H_{max} and $H_{1/3}$ used in the design of model caisson are 75 cm and 55 cm. The submerged depth of the curtain wall is set so as not to receive severe impact air pressure. However, if the submerged depth is too large, the wave power conversion efficiency becomes small. The upper deck height of the turbine room is determined so as not to suffer from water intrusion from the nozzle. The crown height is set to be able to reduce the wave transmission as in conventional breakwaters. These values are determined by a preliminary study and should be examined further. Also, these values should be determined considering the entire wave power conversion system.

Six wave gauges (W1 -W6) were used in the experiments to measure the incident and reflected waves (W1 and W2), the water surface elevation in front of the air chamber (W3), the passing wave in the side flume (W4), the water surface elevation in the air chamber (W5),

and the transmitted waves (W6). Six pressure transducers (P1 - P6) were installed in the model caisson to measure the wave and air pressure. The transducers have a diameter of 10 mm and were fixed in the caisson walls. Only one pressure transducer (P1) was fixed in the front wall and five transducers (P2 -P6) were set in the air chamber. Among them transducers P2 and P3 usually measured the pure air pressure, and the others measured the air pressure plus the wave pressure. Ultrasonic displacement meters (D1 - D3) were also installed to measure the displacement of the caisson. These meters were newly developed to measure the displacement up to 1 m with a resolution of 0.1 mm and 100 Hz.

Irregular waves were used in the experiments. The target wave spectrum was the Bretschneider-Mitsuyasu spectrum(Goda 1985) and the target wave periods $T^*_{1/3}$ were 3.35, 2.24, 1.79, 1.57, and 1.34 s. The water depth h was 97.5 cm. Five wave groups A, B, C , D and E were prepared in the experiments for each significant wave period. Each wave group contained more than 450 waves. The relative water depth ranged from 0.10 to 0.356 and the ratio of the air chamber width to the wave length ranged from 0.036 to 0.128.

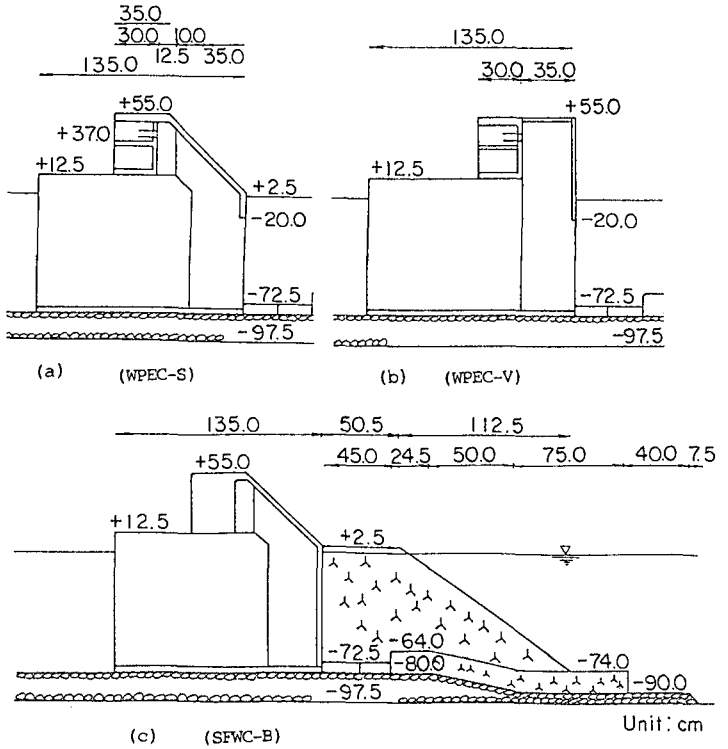

Fig. 2 Cross Sections of Model Caissons

4 FUNCTIONS OF CAISSONS

Conversion Efficiency of the Wave Power Extracting Caissons

The wave power is converted into air power in the air chamber with the nozzle opening ratio set at 0.0075. Figure 3 shows the conversion efficiency of the V-type wave power extracting caisson. The efficiency is from 0.55 to 0.7 where the significant wave height is less than 15 cm. The efficiency is relatively high in this region. The efficiency is lower than 0.5 where the significant wave height is larger than 25 cm, because the wavelength is relatively large and the air leaks from the opening under the curtain wall. The lines in the figure indicate the calculated results. The calculated results agree with the experimental results well.

Figure 4 shows the conversion efficiency for the S-type wave power extracting caisson. The conversion efficiency is changed by the submerged depth of the curtain wall. The efficiency increases with the decrease of the submerged depth clearly where the significant wave height is less than 20 cm. The efficiency of the S-type caisson of d_c = 20 cm is around 70 % where the significant wave height is less than 15 cm. The efficiency for the S-type caisson of d_c = 20 cm in the figure is larger than that for the V-type caisson in Fig 3.

Reflection Coefficient

Figure 5 shows the experimental results of the reflection coefficient of the S-type caisson together with those of the sloped front wall caisson and the caisson with wave dissipating blocks. The reflection coefficient of the S-type caisson is about 0.45 where the wave height is relatively small. The reflection coefficient is about 0.55 even when the wave height is large. The reflection coefficient of the S-type caisson is much smaller than the sloped front wall caisson, but larger than that of the caisson with wave dissipating blocks.

Wave Transmission and Overtopping

The wave transmission coefficients of the four caissons are compared in Fig. 6. For example, the wave transmission coefficient of the S-type caisson is 0.15 when the significant wave height is about 45 cm. The transmission coefficient of the V-type caisson is 0.13 for the same wave height. The transmission coefficient of the S-type caisson is a little larger than that of the V-type caisson. However, the transmission coefficient of the S-type caisson is lower than that of the sloped front wall caisson and is lower than that of the caisson with wave dissipating blocks. When the wave length and height are large, the waves climb up on the wave dissipating blocks. Therefore, the transmission coefficient of the caisson with the wave dissipating blocks is not less than that of the S-type caisson. The wave transmission in the experiments includes the wave transmission through the gap between the model caisson and the flume walls in addition to the wave transmission through the rubble foundation.

It is said that a sloped front wall caisson needs to have a crown

height of 1.0 $H_{1/3}$ to reduce the wave transmission to a level as low as that by an ordinary vertical wall caisson with a crown height of 0.6 $H_{1/3}$. The wave transmission of the S-type caisson with the crown height of 1.0$H_{1/3}$ is probably lower than that of the ordinary vertical caisson with the crown height of 0.6$H_{1/3}$. The wave transmission characteristics of the four caissons can be observed also by the wave overtopping rate although the experimental results are not shown here.

Water Surface Elevation

The maximum and the 1/3 highest values of the water surface elevation η^+ in the air chamber of the S-type caisson are plotted in Fig. 7. The maximum and the 1/3 highest values of $\eta^+/H_{1/3}$ increase with the increase of the significant wave period and decrease with the increase of the significant wave height. The maximum value ranges η^+ from 0.6 to 1.0 $H_{1/3}$ and is above 37 cm when the significant wave

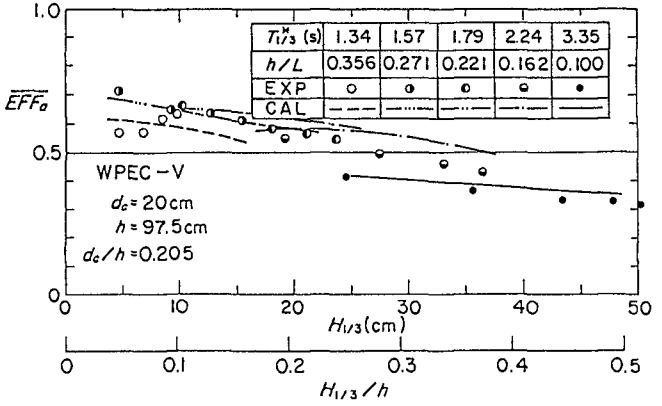

Fig.3 Conversion Efficiency of V-type Caisson

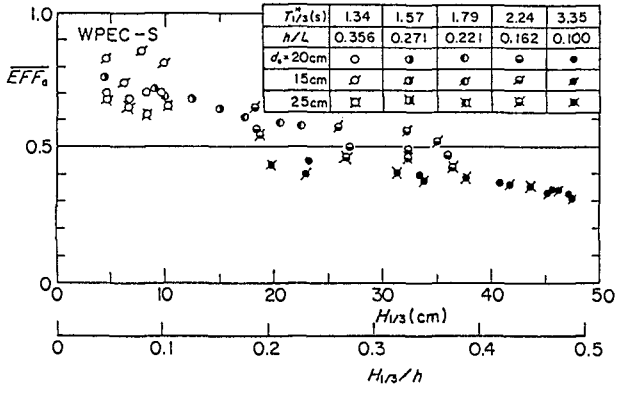

Fig. 4 Conversion Efficiency of S-type Caisson

period is 3.35 s and the significant wave height is larger than 40 cm. The upper deck of the machine room of the caisson is 37 cm above the still water level, which is designed to be $0.5H_{max}$. When the water level goes higher than the upper deck level, the water might intrude into the turbine opening. However, only the waves with a wave height near the maximum wave height can go up above the level and the velocity of the water surface elevation is very small when the water level reaches the upper deck level. It should be noted that the water surface elevation in the air chamber increases with the increase of the nozzle opening ratio.

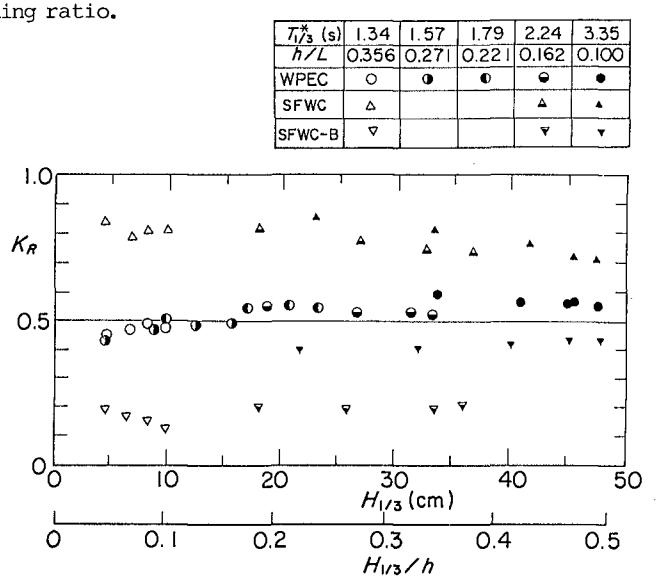

Fig. 5 Wave Reflection Coefficients

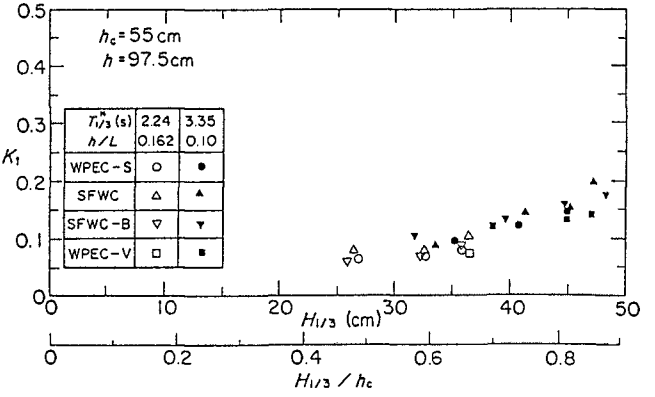

Fig. 6 Wave Transmisson Coefficients

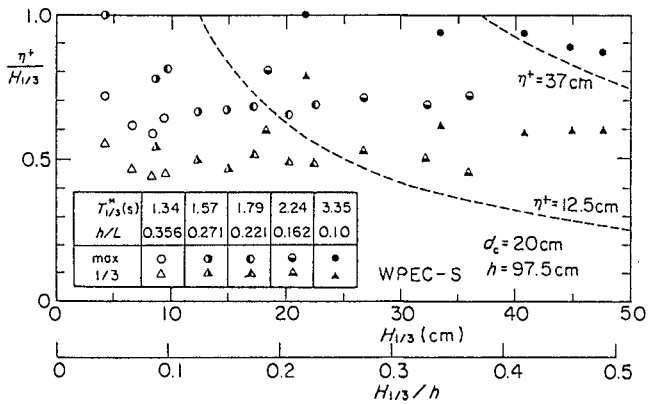

Fig. 7 Water Surface Elevation in the Air Chamber

5. WAVE PRESSURE AND WAVE-INDUCED AIR PRESSURE

Sample Analogue Data

Figure 8 shows sample analogue data when irregular waves of $T_{1/3}$= 3.35 s and $H_{1/3}$= 47.8 cm act on the S-type wave power extracting caisson. The water surface elevations η_F in front of the caisson, η_{pass} in the side channel and η in the air chamber are shown in the figure. The wave pressure p_1 on the sloped wall, the air pressure p_2 in the air chamber and the horizontal displacement R_S of the caisson are also shown in the figure. The air pressure becomes almost zero when the water surface elevation in the air chamber is below the curtain wall depth. Impact air pressure appears when the air in the air chamber is compressed by the uprising water surface. The impact air pressure occurs only when the water surface elevation in front of the chamber goes down significantly below the curtain wall depth. Impulsive pressure also appears on the sloped front wall. This pressure is generated by the direct impact of the water surface of waves and is characterized by its sharp rise and very short duration. Takahashi and Tanimoto (1983) named the air compression pressure Bagnold pressure and the direct wave impact pressure Wagner pressure. Bagnold (1939) and Wagner(1932) gave the theories on these pressures respectively.

Positive and Negative Peak Values of the Air Pressure

Figure 9 shows the positive peak values of the air pressure in the air chamber of the S-type caisson. The value of the air pressure p^+_{23} is the average of the values obtained by the two pressure sensors P2 and P3. The 1/3 highest peak values and the maximum peak values which are divided by $w_oH_{1/3}$ are plotted in the figure. The maximum and the 1/3 highest values of $p^+_{23}/w_oH_{1/3}$ increase with the increase of the significant wave height as a whole. However, the maximum value decreases where the significant wave height is larger than 40 cm. This is because the wave height is limited by the wave breaking. The maximum value fluctuates very significantly, and therefore additional

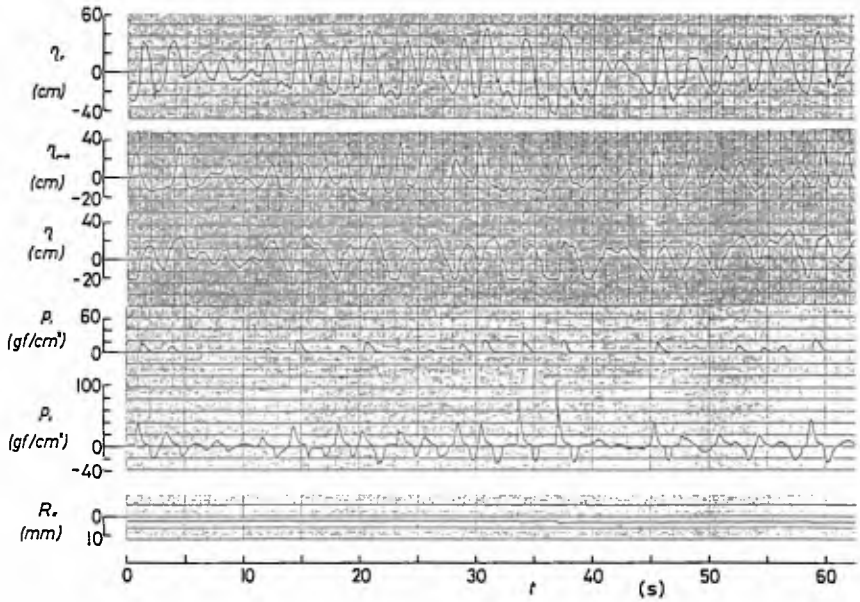

Fig. 8 Sample Analogue Data ($T^*_{1/3}$=3.35s, $H_{1/3}$=47.8cm, WPEC-S)

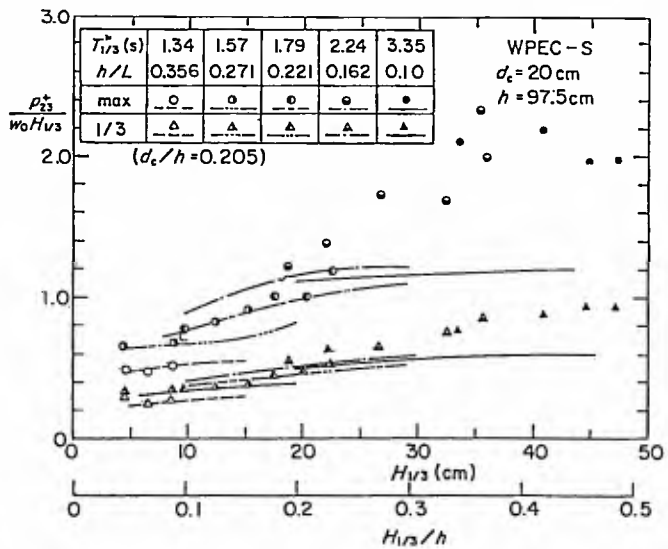

Fig. 9 Positive Air Pressure

measurements were conducted. Even though the incident wave train in the experiment is the same, the maximum value varies greatly. For example, the average of the maximum values for eight repeated measurements is 92.0 gf/cm^2 and their standard deviation is 10.4 gf/cm^2, while the average value of the significant wave height is 47.3 cm and the standard deviation is 0.6 cm. The average of the maximum values is 1.35 w_oH_{max} and equals 1.94 $w_oH_{1/3}$. The calculated value of the air pressure is also shown by the lines in the figure. The calculated value is much smaller when the impact air pressure occurs because the calculation cannot include the impact air compression.

Figure 10 shows the negative peak p^-_{23} of the air pressure. The maximum and the 1/3 highest absolute value of $p^-_{23}/w_oH_{1/3}$ increase with the increase of the significant wave height. However the maximum value decrease and the 1/3 highest value becomes constant when the significant wave height is larger than approximately 20 cm. This is because the water surface in front of the air chamber goes below the curtain wall and then the air pressure becomes the atmospheric pressure. The maximum absolute value of p_{23}^- is 0.50 w_oH_{max} when $T^*_{1/3}$= 3.35 s and $H_{1/3}$= 47.4 cm.

The measurement of the air pressure was also conducted for the V-type caisson. The air pressure of the V-type caisson shows almost the same tendency as that of the S-type caisson. The submerged depth of the curtain wall was changed in the experiments. It was found that the air pressure increases with the decrease of the submerged depth.

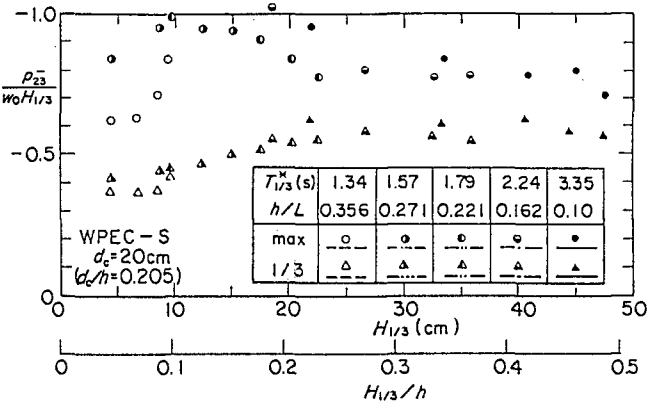

Fig. 10 Negative Air Pressure

Theory of the Impact Air Pressure

The uplift force on the ceiling slab of a wave dissipating caisson is generated by the compression of an air layer by the uprising water surface. This phenomenon is very similar to the impact air compression in the air chamber. The uplift force was investigated by Takahashi and Tanimoto(1985) employing the theory introduced by Bagnold(1939) and extended by Mitsuyasu(1966). The theory comprises

the equation of motion of the effective water mass which compresses the air and the equation of air pressure. The theory can be applied for the impact air compression in the air chamber.

The equation of the air pressure derived by Bagnold assumes an adiabatic air compression. However, the thermodynamic equations used in **2** can also describe the impact air compression even without the assumption of the adiabatic change. That is, Eqs.(1) and (2) express the thermodynamics in the air chamber. Then the water surface elevation can be expressed by the following equation:

$$\rho_w k_e \frac{d^2\eta}{dt^2} = -p^* \tag{9}$$

where, k_e is the thickness of the effective water mass, which is given by

$$k_e = 0.25 \pi B \tag{10}$$

The initial conditions of the equations are given by

$$\left.\begin{aligned} \frac{d\eta}{dt} &= u_o \\ \eta &= -d_c \end{aligned}\right\} \text{ at } t = 0 \tag{11}$$

where u_o is the uprising velocity at t = 0 and $\eta = -d_c$. The initial thickness of the air layer is $d_c + D_o$. The equations mentioned above are almost the same as those in **2** but Eq.(9) instead of Eq.(3) is used. The equations can be solved by step-by-step numerical calculations.

Sample Calculations and Similitude Law

Sample calculations were made for the impact air pressure in the model air chamber. The value of the effective thickness of the water k_e is 27.5 cm, and the initial thickness D_o+d_c of the air layer is 65 cm. For example the peak value of the air pressure p_c becomes 95.8 gf/cm^2 when the uprising water surface speed is 194.4 cm/s and the nozzle opening ratio is 0.0075. The time t_p from the start of the compression to the peak is 0.0457 s in this case.

If the model scale is 1/20, the peak air pressure p_c is 787 gf/cm^2 when the uprising velocity u_o is 8.96 m/s and ε = 0.0075. This means that the the peak air pressure becomes only 7.49 times that for the 1/20 model. The peak impact air pressure is 1/2.43 that predicted by the model experiments. That is, the correction factor λ of the experimental results is 2.43 in this case. This model scale effect comes from the compressibility of the air as described by Takahashi and Tanimoto(1985).

Prediction of the Impact Air Pressure

The impact air pressure for the prototype and model air chamber can be predicted by the calculation mentioned above. The effective thickness of the water mass k_e and the initial thickness of the air are evaluated by the dimensions of the air chamber. Estimation of the

uprising velocity of the water surface is very difficult. However the maximum value of the uprising velocity in the experiment can be roughly estimated by the following procedure:

a) The maximum absolute value of negative peak of water surface elevation $|\eta^-_{pass}|$ is given by the wave height $H_{1/3}$ for incident wave train as follows:.

$$\left|\left(\frac{\eta^-_{pass}}{H_{1/3}}\right)\right|_{max} = -1.2\frac{H_{1/3}}{h} + 1 \quad : H_{1/3} < 0.417h \qquad (12)$$

$$= 0.5 \quad : H_{1/3} \geq 0.417h$$

b) The maximum absolute value of the water surface elevation in front of the air chamber $|\eta^-_F|$ is obtained from $|\eta^-_{pass}|$ as follows:

$$|(\eta^-_F)|_{max} = 1.4|(\eta^-_{pass})|_{max} \quad : |(\eta^-_{pass})|_{max} < d_c/1.4$$

$$= 3.5|(\eta^-_{pass})|_{max} - 30 \quad : d_c/1.4 \leq |(\eta^-_{pass})|_{max} < d_c \qquad (13)$$

$$= 2.0|(\eta^-_{pass})|_{max} \quad : |(\eta^-_{pass})|_{max} \geq d_c$$

c) The maximum value of the uprizing velocity u_o is given by $|\eta^-_F|$ as follows:

$$u_0 = \sqrt{g|\eta^-_F|}\{1-(d_c/|\eta^-_F|)^2\}^{1/2} \qquad (14)$$

The calculated values by the above procedure agree with the experimental value as a whole. However, Eqs(11),(12) and (13) are only derived from the experimental results. Further study should be made to confirm the above procedure.

6. DESIGN OF CAISSON

Design of the Walls in the Air Chamber

The walls in the air chamber including the curtain walls should be designed against the wave and wave-generated air pressure. The following three phases should be considered in the design:

a) Peak of the positive air pressure
The impulsive air pressure can be calculated by the procedure described in 5. It should be noted again that the prototype value becomes much smaller than that predicted from the model value. If the impact air pressure is small, the slowly-varying air pressure is important for the design. The value 1.0 w_o H_{max} in the figure is recommended for prototype air chambers of ordinary size and with an ordinary nozzle opening ratio. It should be noted that the impact pressure may exceed 1.0 H_{max} when the air chamber is small and the wave height is small.

b) Peak of negative air pressure
The value of 0.5 $w_o H_{max}$ is recommended for ordinary air chambers. This is a conservative value. The negative air pressure is not impulsive.

c) Peak of impulsive wave pressure
When the impulsive wave pressure acts on the front walls the air pressure is still positive. However the air pressure becomes relatively small for the prototype air chamber. Therefore, the air

pressure can be assumed to be zero when the impulsive air pressure acts. The value of 1.0 $w_o H_{max}$ is recommended for the impulsive wave pressure on the front wall.

Stability Design of the Caisson

Goda proposed a wave pressure formula for the upright section of vertical breakwaters, which is now a standard formula for the caissons of composite breakwaters. The formula can be applied even for the wave power extracting caissons with a little modification. That is, the coefficient α_2 in the Goda formula is set to be zero for the wave power extracting caissons because the caissons absorb the wave energy. (For details, see Goda 1985 pp.107 - 144.)

When the front face of the caisson is inclined as the S-type caisson, the wave pressure on this part contributes to the forces in the horizontal direction and in the vertical direction. This vertical force acts downward and increases the stability of the caisson. The vertical force P_{sv} and the horizontal force P_{sh} are usually defined as follows:

$$\begin{aligned} P_{sh} &= P_s \sin^2\theta_s \\ P_{sv} &= 0.5\, P_s \sin 2\theta_s \end{aligned} \qquad (15)$$

where θ_s is the angle of the inclination of the sloped wall and P_s is the wave force above the beginning of the sloped wall.

Results of the Sliding Tests of the Caissons

Sliding Tests of the caissons were conducted to examine the pressure formula and to compare the stability of the caissons. The weight of the caisson was changed and the sliding distance of the caissons was measured. It can be concluded that the application of Goda's pressure formula with the modification is valid for the caissons examined in the experiments. The weight needed to stabilize the caisson changes greatly depending on the shape of the caisson. The S-type wave power extracting caisson requires less weight than the V-type wave power extracting caisson and than the sloped front wall caisson.

7. CONCLUSIONS

The functions and stability of the wave power extracting caisson breakwaters are investigated experimentally. Two wave power extracting caissons are tested in the experiments. One is the wave power extracting caisson with the sloped front wall (the S-type caisson) and the other is the caisson with the vertical front wall (the V-type caisson). However the S-type caisson is mainly discussed. Other caissons such as a sloped front wall caisson and a sloped front wall caisson with wave dissipating blocks are also tested in the experiments for comparison. Major conclusions are as follows:

1) The wave power extracting caisson can convert wave power into air power with relatively high efficiency, and the wave power extracting

caisson has low wave reflection and low wave transsmision characteristics.

2) Large impact air pressure occurs in the model air chamber of the wave power extracting caisson. The calculation method of the impact air pressure is presented. The impact air pressure in the prototype air chamber predicted by the calculation is much smaller than that evaluated with the Froude similitude law from the experimental result.
3) The pressure distribution for the design of the walls of the air chamber is proposed. The pressure distribution for the stability design of the S-type wave power extracting caisson is proposed, which is confirmed by the sliding tests of the caisson.
4) The stability of the S-type caisson against storm waves is high compared with other caissons.

The First Port Construction Bureau of the Ministry of Transport has decided to conduct field experiments of the wave power extracting caisson breakwater in Sakata Port from fiscal 1987 to 1991. A prototype wave power extracting caisson breakwater will be installed with a turbine and a generator.

The author wishes to express his deep appreciation to Dr. Y. Goda, Mr. T. Asada and Dr. K. Tanimoto for their precious comments on the present study.

REFERENCE

Bagnold, M.R.A.(1939): Interim report on wave pressure research, Jour. of Institute of Civil Engineers, Vol.12, pp.201 - 226.

Goda, Y.(1985): Random Seas and Design of Maritime Structures, Univ. of Tokyo Press.,322p.

Jarlan, G.E.(1961): A perforated vertical wall breakwater, Dock and Harbour Authority, pp.394 - 398.

Mitsuyasu, H.(1966): Shock pressure of breaking wave, Proc. of 10th Conference on Coastal Engineering, pp.268 -283.

Ojima, R., Suzumura,S., and Goda, Y.(1984): Theory and experiments on extractable wave power by an oscillating water-column type breakwater caisson. Coastal Engg. in Japan, Vol.27, pp.315- 326.

Takahashi, S.,Tanimoto, K., and Suzumura, S.(1983): Generation mechanism of impulsive pressure by breaking waves on a vertical wall, Rept. of Port and Harbour Res. Inst., Vol. 22, No.4. pp.3 - 31, (in Japanese).

Takahashi, S., and Tanimoto,K(1985): Uplift forces due to compression of enclosed air layer and their similitude law, Coastal Engineering in Japan, Vol.28, pp.191 -206.

Takahashi, S., Suzumura,S., and Myose, K.(1986): Turbine power by wave power extracting system with vertical breakwaters, Proc. of 5th OMAE Conference, ASME, pp.553-559.

Takahashi, S.,Myose,K., Yoshimoto,Y., and Tanaka, S.(1987): Variation of wave power extraction due to incident angle and directional wave spreading. Rept. of PHRI, Vol.26, No.3. pp.3-39.

Wagner, H.(1932): Über Stoss-und Gleitvorgänge and der Oberfläche von Flussigkeiten, Zeishrift für Angewandte Mathematik und Mechnik, Band 12, Heft 4, pp.193 -215.